Radiat Environ Biophys (1994) 33:353–364

Radiation and Environmental Biophysics

Calibrating and testing tissue equivalent proportional counters with ^{37}Ar

E. Anachkova [1], A.M. Kellerer [1,2], H. Roos [1]

[1] Strahlenbiologisches Institut der Universität München, Schillerstrasse 42, D-80336 München, Germany
[2] Institut für Strahlenbiologie, GSF-Forschungszentrum, Postfach 1129, D-85758 Oberschleißheim, Germany

Received: 21 March 1994 / Accepted in revised form: 22 June 1994

Abstract. A method for testing and calibrating tissue equivalent proportional counters with ^{37}Ar is described. ^{37}Ar is produced by exposure of argon in its normal isotope composition to thermal neutrons. It is shown that – up to volume ratios of 0.01 of argon to the tissue equivalent gas – there is no appreciable effect of the argon admixture on the function of the proportional counter. Conventional calibration methods with characteristic x-rays or with α-particles require modifications of the detectors, and they test only small sub-volumes in the counters. In contrast, argon permits calibrations and tests of the resolution that are representative for the entire counter volume and that do not require changes in detector construction. The method is equally applicable to multi-element proportional counters; it is here exemplified by its application to a long cylindrical counter of simplified design that is part of such a multi-element configuration.

Introduction

Radiation protection measurements with proportional counters are well suited to meet the requirements of increased precision and accuracy that have resulted from tightened dose limits and from the increase of the quality factors for neutrons (ICRP 1991). The applicability of proportional counters has been broadened, because the variance-covariance method (Kellerer and Rossi 1984) permits determinations of radiation quality in fields of higher dose rates and in the pulsed fields of accelerators, while multi-element counters, as conceived and tested by Rossi et al. (Kliauga et al. 1987; Rossi 1983), can extend the applicability of tissue equivalent (TE) proportional counters to the low-dose rates that are encountered in neutron measurements. The wide range of applicability corresponds to a broad variety of constructions, and this poses problems of testing and calibrating the instruments that often cannot be solved with the methods conventionally used in microdosimetry (ICRU 1983). To overcome this problem,

Correspondence to: E. Anachkova

we have gone back to a calibration procedure with ^{37}Ar, which was used previously for the development of proportional counters (Hanna et al. 1949), and which has also been employed in early microdosimetric studies by Rossi (see Rossi 1984). While the method is of general applicability, it will be presented here in its application to small cylindrical counters that are part of a multi-element system designed for radiation fields with neutrons.

Problems with the familiar calibration procedures

External radiation fields produce broad energy spectra of charged secondaries in TE proportional counters, and these secondaries, in turn, deposit largely different energies in the counter. The resulting microdosimetric spectra provide the characteristic information to determine the quality of the radiation field (ICRU 1986), but the spectra always extend over several orders of magnitude in pulse height, and they do not have features that permit the recognition of slight variations in the response of the detector. If the measurements in neutron fields are performed with spherical counters, it is usually possible to recognize the position of the proton edge, which corresponds then to a lineal energy, y, of about 150 keV/μm (see Dietze et al. 1984), but otherwise there are few possibilities to judge the spectra without special procedures to calibrate pulse height versus energy imparted.

An exception involves measurements with low-energy characteristic x-rays. They release, when they interact with the counter gas, electrons of known energy. At energies up to a few keV, the electrons tend to be fully stopped in the gas, so that one registers the response of the counter to a known and fixed energy. Accordingly, characteristic x-rays are frequently used for testing and calibrating TE proportional counters. The use of low-energy characteristic x-rays is, however, severely limited because they are weakly penetrating. At the dose rates achievable, it is necessary to provide a thin entrance window to the counter. In addition, the method permits a test of only a part of the counter volume, depending on the geometry of the counter, the window, and the x-ray source. For large TE counters which can be easily and reproducibly constructed, the above restrictions are tolerable; for small counters they tend to exclude the use of characteristic x-rays for testing and calibration.

An alternative to characteristic x-rays is the use of a collimated α-ray beam. This method shares the advantages and disadvantages of the use of characteristic x-rays. It is well suited for larger counter constructions, but it is of limited applicability if small counters – and especially larger numbers of small counters – are to be tested and calibrated. In an assemblage of multiple small counters, the use of characteristic x-rays or of α-rays becomes entirely impracticable.

For completeness one may mention the calibration and testing of TE proportional counters by the release – through a UV micro-beam – of single electrons off the inside counter wall. This method has been successfully employed in studies of proportional counter resolution (Curan et al. 1949) as well as in earlier microdosimetric investigations (Kellerer 1968; Srdoc 1979), but it is too complex to be used routinely.

The use of ^{37}Ar for testing and calibration

The admixture of a suitable radionuclide to the counter gas is a far simpler alternative to test and calibrate proportional counters. Among all available radionuclides, ^{37}Ar is the ideal candidate for this purpose. It is an Auger electron emitter with an energy release of roughly 2.8 keV for K-shell capture and 200 eV for L-shell capture. These two energies are very suitable for calibration of counters at simulated site diameters of fractions of a micrometer and more. The half-life of 35.02 days (Lederer and Shirley 1978) of ^{37}Ar is also very convenient; it is sufficiently long for prolonged studies and sufficiently short to minimise problems of counter contamination. ^{37}Ar has, indeed, been used for calibration of proportional counters that used argon as the counting gas (Hanna et al. 1949). It has also – as pointed out by Rossi (1984) – been employed in early microdosimetric studies, but it has not been used subsequently in microdosimetric measurements. The following considerations will show its convenient applicability and its potential for testing and calibrating TE counters. The decay characteristics of ^{37}Ar and the conditions for its production will be discussed, and its applicability will be exemplified through results obtained with a cylindrical TE proportional counter.

Decay characteristics and energy release of ^{37}Ar

With a half-life of 35 days, ^{37}Ar transforms by electron capture to stable ^{37}Cl (ICRP 1983; Lederer and Shirley 1978). The probabilities for K-shell and L-shell capture are roughly 0.91 and 0.09 (Lederer and Shirley 1978). The probability of M-shell capture can be disregarded in the present context. The relative probabilities for the release of electrons and photons per nuclear transformation and their energies have been calculated by several authors (Coghlan and Clausing 1973; ICRP 1983; Larkins 1977). Asplund et al. (1977) have measured the KLL and KLM Auger spectra of argon, and Auger electron and x-ray spectra of chlorine in different gaseous compounds have also been measured (Aitken et al. 1980). On the basis of the available information, we have compiled in Table 1 the distribution of Auger electrons and of x-rays that results from the decay of ^{37}Ar. The resolution time of proportional counters is much longer than the decay time, and one measures therefore simultaneously the contribution of the different electrons and photons that are emitted due to a decay. Part of the

Table 1. Radiation yields and the corresponding energies from the decay of ^{37}Ar

Decay mode	Radiation	Electrons	Photons	Yield per decay
K-capture	Auger KLL	2.38 keV	200 eV	0.738
	Auger KLM	2.6 keV	200 eV	0.0837
	Auger KMM	2.8 keV		0.0047
	Kα x-ray		(2.6 keV), 200 eV	0.0795
	Kβ x-ray		(2.8 keV)	0.0064
L-capture	Auger LMM	193 eV		0.09
	Lα x-ray		208 eV	0.0003
	Lβ x-ray		260 eV	0.00002

released energy may leave the sensitive volume of the counter. The mean free path of the 2.6 or 2.8 keV photons in TE gas corresponds to more than 50 μm (Seltzer 1993). At the simulated sites – which are considerably smaller – they will, thus, usually escape, and they are therefore listed in parentheses in Table 1. Apart from these photons – that are irrelevant in the present context – the total energy release amounts to 2.8 keV with probability 0.83, and 200 eV with probability 0.17. The mean free path of a 200 eV photon in the TE gas corresponds to about 1 μm (Hubbel 1977). Only part of these photons will, therefore, be registered. The CSDA ranges for 2.4 and 2.6 keV electrons are about 0.2 μm and 0.22 μm (Waibel and Grosswendt 1992). These electrons are likely to deposit all their energy in the sensitive volume of the counter, but an increasing part of the energy of the electrons will be lost when the counter simulates tissue regions less than about 1 μm, i.e. the upper peak will shift to lower energies. The CSDA range of 200 eV electrons is only 6 nm (Waibel and Grosswendt 1992), so that – at the site sizes that are simulated – they will always be contained in the collection volume of the counter.

Production of ^{37}Ar

Among the various reactions for production of ^{37}Ar (Erdtman 1976; Lederer and Shirley 1978), the most convenient one is irradiation of natural argon with thermal neutrons. The ambient abundance (in atom numbers) of the argon isotopes ^{36}Ar, ^{38}Ar and ^{40}Ar is 0.337%, 0.063% and 99.59%. The activation processes, their thermal neutron cross-sections and the resulting relative yields in ambient argon are:

$^{36}Ar(n, y)^{37}Ar$(*half-life* 35 *d*), 5 *barn*, 0.025
$^{38}Ar(n y)^{39}Ar$(*half-life* 269 *y*), 0.8 *barn*, 0.00074
$^{40}Ar(n, y)^{41}Ar$(*half-life* 1.83 *h*), 0.66 *barn*, 0.974

The cross-section for creating ^{37}Ar in this way is small, but the reaction obviates the need for the subsequent chemical separation that arises with other production methods that have a larger cross-section.

At the research reactor FRM at Garching (Technical University of Munich), an in-core position is used with neutron fluence rates $6.6 \cdot 10^{13}$, $4.3 \cdot 10^{12}$ and $3.0 \cdot 10^{13}$ cm^{-2} s^{-1} for thermal, epithermal and fast neutrons, respectively. The epithermal and fast neutrons do not contribute appreciably (Erdtman 1976). The projected new reactor, FRM II, at Garching is to provide a neutron fluence rate that is 50 times larger, but even under the present conditions sufficient activities of ^{37}Ar are readily obtained.

Argon at atmospheric pressure is enclosed in a 8 ml quartz ampoule that is, in turn, encapsulated in an aluminium cylinder. After 5–10 days of irradiation and a subsequent storage time of 5–9 days, the ^{41}Ar has disappeared, and an activity of about 4–9 MBq of ^{37}Ar remains. The only measurable remaining radiation outside the ampoule is that of trace elements in the quartz. The remaining activity is below the exemption level of radiation protection regulations, but it is amply sufficient for the testing and calibration of proportional counters.

Sensitivity of the counter operation to the admixture of argon

Testing and calibration with ^{37}Ar will here be exemplified in its application to TE cylindrical counters under varying operational conditions. The counters are operated with methane-based TE gas (ICRU 1983) at an automatically controlled flow rate. Flow rates of about 7 ml/h (normalised to 1 bar) were employed in the present study. Since the proportion of ^{37}Ar in the ampoule is minuscule, one needs to administer an amount of argon that might affect the gas multiplication of the counter. It is, therefore, important to determine the relative concentration of argon that leaves the operation of the counter unaffected. For convenience, we first studied this question with a standard right cylindrical counter (length and diameter of the counting volume 20 mm) which has a built-in α-ray calibration source. At the simulated site diameter of 1 μm and at an operation voltage of 900 V, we obtained the dependence of the gas gain on the argon concentration that is presented in Fig. 1. Argon with a mass impurity of 10^{-5} was used for this experiment. The volume ratio of argon and TE gas in the gas mixture was determined by the measurement of pressures with an accuracy of 3×10^{-5}. Up to volume ratios of 0.01–0.02, the gas multiplication factor remains constant within 3%–4%, followed by a certain increase. With argon that has been irradiated in the quartz ampoule, no increase of gas multiplication is seen up to a volume ratio 0.01 of argon, and with higher admixtures of argon, the gas multiplication actually decreases somewhat; this effect might be caused by impurities in the argon from the quartz ampoules or from the procedure of filling and heat sealing the ampoules. The essential conclusion is that the counter operation remains unaffected at volume ratios of argon up to 0.01.

Calibration

Pulse height spectra for ^{37}Ar were obtained with the standard (20×20 mm) cylindrical counter and with a smaller counter which is a prototype for a multi-element detector. The prototype has a simple cylindrical geometry. Its length is 60 mm, its diameter 3 mm, and no guard electrodes are utilized; it is, therefore, a good example of an instrument that cannot be readily tested or calibrated by the usual methods, while it demands testing because of its uncommonly simple design. The results for this counter will, therefore, be presented in detail.

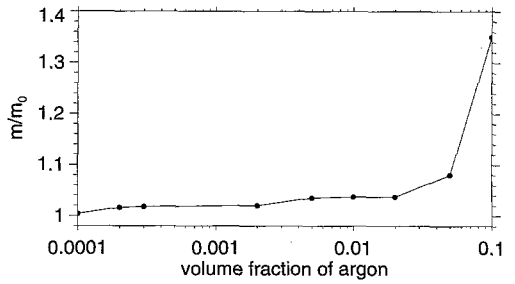

Fig. 1. Dependence of the gas multiplication in tissue equivalent (TE) gas on the volume fraction of admixed argon. The dependence is given relative to the gas multiplication in pure TE gas. Simulated diameter 1 μm, operation voltage 900 V

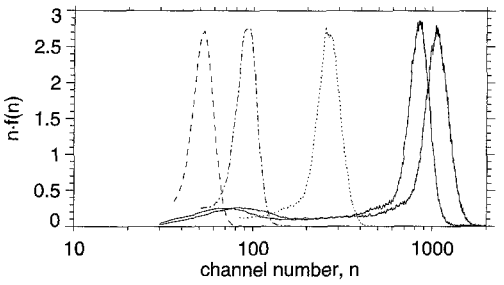

Fig. 2. Pulse height spectra at 1 μm simulated diameter, different detector voltages, and electronic *gain*. From *left* to *right*: 900 *V*, *gain* 10; 800 *V*, *gain* 50; 1100 *V*, *gain* 5; 1000 *V*, *gain* 50; 1100 *V*, *gain* 20

At a given argon concentration the observed count rate depends on the counter volume and on the pressure. At a volume ratio of 0.01, the pulse rate in the small counter was of the order of 5 and 50 s^{-1} at simulated site diameters of 0.2 μm and 2 μm, respectively. These values apply to the specific activity of ^{37}Ar that is reached by the neutron exposure times and conditions specified above. At a gas flow rate of 7 ml/h (normalised to 1 bar) and at an argon volume ratio of 0.01, one ampoule of neutron-exposed argon suffices for up to 100 h of continuous operation of the TE counter.

The pulse height spectra in Fig. 2 are taken at a simulated diameter of 1 μm. A logarithmic abscissa scale is used to accommodate the broad range of pulse heights that results with different voltages and different electronic gain. To preserve the area in the logarithmic scale, the pulse frequencies – initially determined on a linear scale in the analogue-digital converter – are multiplied by the channel numbers, i.e. the density relative to the logarithmic scale is plotted.

For calibration in terms of the K-capture peak, one must assign the central value of this peak to the central value, ε_k, of the energy imparted due to the K-capture events. This imparted energy has its main contribution from the electrons that tend – at simulated diameters of 1 μm or more – to be fully absorbed in the collecting volume. Their mean contribution per event is then 2.405 keV. A smaller contribution is due to the accompanying 200-eV photons; this amounts on average to 377 eV energy per K-Auger event times the absorbed fraction, f, which depends on the mean free path of the photons and the cylinder geometry:

$$\varepsilon_k = 2.405\ \text{keV} + f \cdot 0.377\ \text{keV}. \tag{1}$$

The absorbed fraction, f, of the photons can be calculated from

$$f = \int_0^{x_{max}} \lambda_0 e^{-x/\lambda_0} U(x)\,dx, \quad (x_{max} = \sqrt{d^2 + h^2}) \tag{2}$$

where $U(x)$ is the geometric reduction factor for the simulated cylinder and λ_0 is the mean free path of the photon. The formula for $U(x)$ is given in NCRP Report 108 (1991) (see Eqns. C.10–C.12). Figure 3 gives the absorbed fraction as a function of d/λ_0 for the cylinder of equal height and diameter ($h = d$) and for the cylinder of elongation 20 ($h = 20d$). The dependence for the elongated cylinder is virtually identical to that for an infinite cylinder.

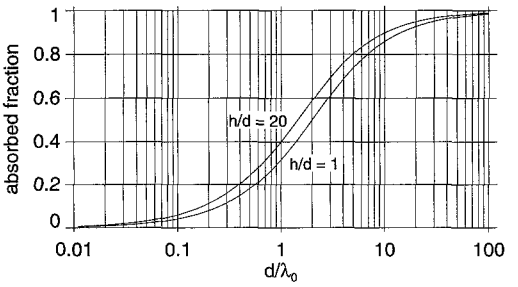

Fig. 3 Fraction of absorbed photons in cylinders with two different elongations. *Abscissa* is the ratio of the cylinder diameter, d, to mean free path, λ_0, of the photon

Hubbel (1977) gives the value 1 μm (scaled to the density of tissue) for the mean free path of the 200 eV photons in methane-based TE gas. With this value one obtains from Fig. 3 the absorbed fractions 0.6, 0.4 and 0.25 for the simulated diameters 2 μm and 0.5 μm, respectively. This corresponds, according to (1), to the central values 2.63 keV, 2.56 keV and 2.5 keV of the energy imparted. In the measured spectra the peaks corresponding to the K-shell events are fitted to normal distributions to determine their central values that are then, for the simulated diameters 2 μm and 1 μm, assigned the values 2.63 keV and 2.56 keV. For smaller simulated diameters the calibration is more complicated, because one needs to account for incomplete energy deposition by some of the Auger electrons.

The complexity of the partial excape of electron energy suggested a direct determination for smaller simulated diameters, and this was achieved by measuring the argon spectra in the larger 20×20 mm cylindrical proportional counter and comparing it with earlier calibrations in terms of a built-in ^{241}Am α-source (Chen 1991). This procedure has provided energy values that are consistent with the computed energies for the diameters 2 μm, 1 μm and 0.5 μm; they are listed in the first column of Table 2. Since the intercalibaration did not aim at high precision, the values must be considered approximate.

Detector resolution

With the calibration values of Table 2 one obtains the distributions in Fig. 4. It can be seen that the resolution changes little over a wide range of gas multipli-

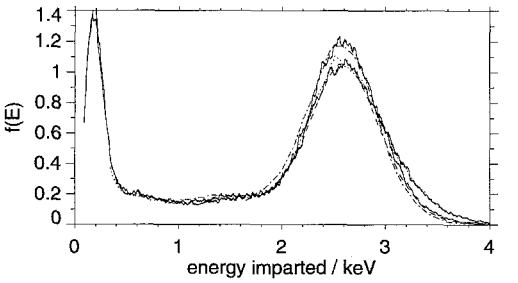

Fig. 4. Single event distributions at simulated diameter 1 μm. The spectra are the same as in Fig. 2 but are given on a linear energy scale. The normalization includes only the K-peak

Table 2. Energy resolution characteristics of the prototype counter

Simulated diameter (μm)	K-peak position (keV)	Electronic gain	Voltage (V)	σ/ε_K [a]	FWHM (keV)	FWHM/ε_K
2	2.63	50	1000	0.134	0.80	0.317
		20	1050	0.123	0.74	0.29
		20	1100	0.118	0.72	0.29
1	2.55	50	800	0.122	0.74	0.288
		10	900	0.127	0.79	0.30
		50	1000	0.12	0.73	0.285
		5	1100	0.127	0.79	0.30
0.5	2.5	50	700	0.114	0.67	0.27
		50	800	0.114	0.68	0.27
		20	900	0.118	0.69	0.28
0.3	2.4	20	700	0.114	0.65	0.27
		20	800	0.11	0.62	0.26

[a] Values derived from fit of the peak to a Gaussian distribution
FWHM, full width at half-maximum; σ, standard deviation; ε_K, central energy

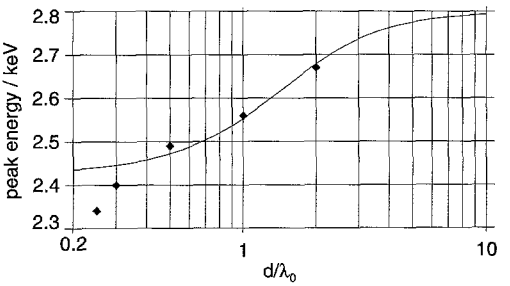

Fig. 5. Dependence of the position of the K-peak on the ratio of the simulated diameter to the mean free path of the photon. The *line* gives the computed values that do not account for escape of electron energy. The points give values derived from an intercalibration with α-rays

cation. Table 2 gives – for the Gaussian distributions fitted to the K-peak – the relative standard deviations σ/ε_k, i.e. the standard deviations, σ, divided by the central energy, ε_k. The full width at half-maximum (FWHM) divided by the mean is frequently used as a parameter of the counter resolution; the values of this ratio are read from the observed spectra and are also given in Table 2; they agree closely with the values $2.36\sigma/\varepsilon_k$ of the fits to Gaussian distributions.

To judge the performance of the counter, one needs to compare the observed resolution with the values that could ideally be reached. For this purpose one needs to consider the various factors that contribute additively (Kellerer 1968) to the relative variance, $V_r = \sigma^2/\varepsilon_k^2$, of the calibration spectrum.

Variations of energy imparted. For the K-peak one can have the imparted energies of 2.4 keV, 2.6 keV or 2.8 keV. To compute the relative variance one can make the somewhat simplified – but uncritical – assumption that in the 2-photon event the probability for absorbing no photons, one photon or both photons is $(1-f)^2$, $2\cdot(1-f)\cdot f$, and f^2, respectively. With this assumption one obtains the positions of the K-peak (Fig. 5) and the relative variance, V_1 (Fig. 6). The maximum relative variance $V_1 = 0.0053$ occurs at $f = 0.45$, i.e. at simulated diame-

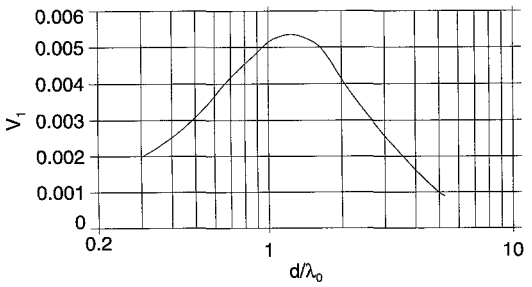

Fig. 6. The relative variance, V_1, of energy imparted due to K-events, with no accounting for the escape of electrons

ter of 1.2 μm. It will be seen that V_1 is smaller than the variance that is due to the two subsequent factors, the Fano fluctuations and the multiplication statistics.

For smaller diameters the K-peak broadens and shifts towards lower energies, because increasing parts of the electron tracks leave the counter volume.

For the L-peak, which is most important for calibration at smaller simulated diameters, the 193 eV LMM-Auger electron is dominant, and V_1 can, therefore, be disregarded.

Fluctuation of the number of ions. Even for a fixed imparted energy, the initial number of ionizations varies; this is referred to as Fano fluctuations (Fano 1947). As Fano has pointed out, the relative variance of the number of ionizations is roughly half of the value that applies for a Poisson distribution, i.e. it equals $V_2 = w/2\varepsilon$, where w is the mean energy per ionization and ε is the electron energy.

Multiplication statistics. Fluctuations are also introduced by the statistics of the gas multiplication process. This factor has, in earlier studies, been elucidated by measurements of the distribution of pulse heights, x, due to single electrons (Curan et al. 1949; Kellerer 1968; Srdoc 1979). In optimal cases the distribution was of the form $x \cdot \exp(-2x/x_0)$, where x_0 is the mean pulse height. The contribution V_3 to the variance is then – as can be readily shown – equal to $w/2\varepsilon$, i.e. one has $V_2 + V_3 = w/\varepsilon$, and one can then represent the distribution of pulse heights by a gamma-distribution which is the λ-fold convolution of $\exp(-x/x_0)$ (Kellerer 1968):

$$\exp(-x/x_0)^{*\lambda} = c \cdot x^{\lambda-1} \exp(-x/x_0) \quad \text{where } \lambda = \varepsilon/\mathrm{w} \tag{3}$$

Non-uniformities of gain. For an ideal counter the gain would not depend on the position of the primary ionisation within the sensitive region. In reality, there are variations that depend on the counter design and that could be substantial for a counter without guard electrodes and without a field shaping helix around the central wire. The contribution, V_4, to the relative variance needs to be inferred from the difference between the observed total relative variance, V_r, of the calibration spectrum and the above contributions V_1, V_2 and V_3.

The best Gaussian fit to the experimental pulse height spectra at simulated diameter 1 μm and at voltage 1000 V has a value of 0.73 keV for the FWHM (29% of the central energy, 2.56 keV); the corresponding relative variance is

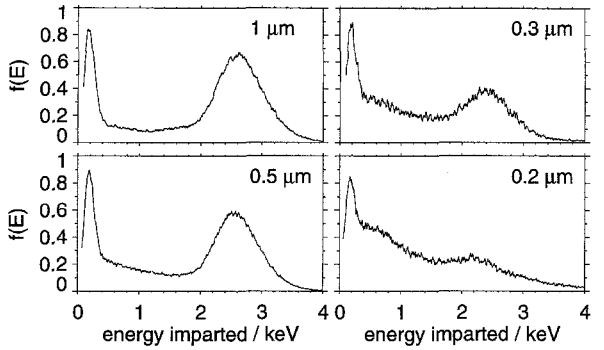

Fig. 7. Single event distributions of energy imparted at different simulated diameters. The normalization pertains to the entire spectra

$V_r = 0.016$. If one assumes the value $w = 29.8$ eV (Waibel and Grosswendt 1992) and $V_1 = 0.005$, one expects a combined contribution, $V_1 + V_2 + V_3$, of the Fano fluctuations and the multiplications statistics of $V_1 + w/\varepsilon_K = 0.016$. The observed values are close to 0.015, i.e. one concludes that the observed resolution is nearly equal to that of a counter with uniform response and with the optimal pulse distribution $\sim x \cdot \exp(-2x/x_0)$ for single ions. An influence of spatial non-uniformity might exist, but it must be small. It may appear surprising that a very simple counter would exhibit no appreciable influence of the spatial non-uniformity of sensitivity. However, the length of the counter explains the lack of influence of field inhomogeneties at the counter ends. On the other hand, there is no need for a field shaping central helix, because the multiplication region is a very small fraction of the sensitive volume; a calculated multiplication profile shows that the multiplication region extends – under the above operational conditions – to a radius of only 40 μm, which corresponds to a fraction of only 0.07% of the counter volume.

Figure 7 represents the calibration spectra at decreasing simulated diameters. At smaller simulated diameters a considerable part of the energy released in the K-shell events escapes the sensitive volume of the counter, and the L-shell contribution becomes correspondingly more prominent.

The low-energy peak is close to noise. To observe it entirely, one requires high gas gain and low noise. The spectra in Fig. 8 are obtained under these conditions; they are well represented by the gamma-distribution:

$$f(x) = c \cdot e^{-x} \cdot x^{\lambda - 1}$$

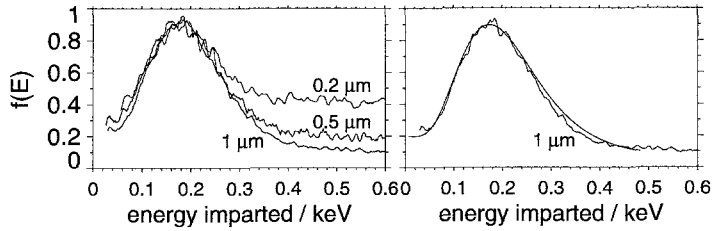

Fig. 8. Single events distributions in the region of L-peak at different simulated diameters (*left panel*) and comparison of the spectrum for 1 μm with a fit in terms of a gamma-distribution superimposed on the tail of the K peak (*right panel*)

that corresponds to (3). In this equation λ is the mean number of ionizations, and the best fit is obtained with $\lambda = 6 \pm 0.5$, which corresponds to $w = 32.2 \pm 2.7$ eV. The relative variance for this distribution is $V_r = 1/\lambda = 0.166$.

Conclusions

^{37}Ar obtained by irradiation of natural argon with thermal neutrons can – by admixture to TE gas – be conveniently used for the testing and calibration of TE proportional counters. The use of this method offers a variety of advantages. It requires no technical modifications in the detectors. ^{37}Ar is uniformly distributed throughout the counter volume, and the calibration factor that one obtains is, therefore, representative for the whole volume, and not only for part of it, as would be the case for other calibration procedures. Two calibration lines with quite different energies are available, and the calibration is thus possible at simulated diameters of fraction of a micrometer and more. For small counters that do not admit built-in calibration probes, the method is essential, and it is equally essential for multi-element counters. In addition to the calibration factor, one obtains information about counter resolution, noise and electrical stability, which can be essential in the construction and testing of TE proportional counters.

Acknowledgements. We are greatly indebted to Dr. F.-M. Wagner, Research Reactor Garching of the Technical University Munich, for performing the neutron irradiations of the argon samples and for profitable scientific discussions. Valuable advice was given by Prof. H.H. Rossi. This work was performed in co-operation with EURADOS Working Group 10, and it was supported by EURATOM contract FI3P-CT20039.

References

Aitken EJ, Bahl MK, Bomben KD (1980) Electron spectroscopic investigations of the influence of initial- and final-state effects on electronegativity. J Am Chem Soc 102:4874–4882

Asplund L, Kelfve P, Siegbahn H, Siegbahn K (1977) Argon KLL and KLM Auger electron spectra. Physica Scripta 16:268–272

Chen J (1991) Mikrodosimetrie in variierenden Strahlenfeldern. Entwicklung der Varianz-Kovarianz Methode. Dissertation, Universität Würzburg

Coghlan WA, Clausing RE (1973) Auger Catalog. Atomic Data 5:317–469

Curan CS, Cockroft AL, Angus J (1949) Investigation of soft radiation by proportional counters. Phil Mag 40:929–937

Dietze G, Menzel HG, Bühler G (1984) Calibration of tissue equivalent proportional counters used as radiation protection dosimeters. Radiat Prot Dosim 9:245–249

Erdtman G (1976) Neutron activation tables. Verlag Chemie, Weinheim

Fano U (1947) Ionization yield of radiations. II. The fluctuations of the number of ions. Phys Rev 72:26–29

Hanna CG, Kirkwood DHW, Pontecorvo B (1949) High multiplication proportional counters for energy measurements. Phys Rev 75:985–986

Hubbel JH (1977) Photon mass attenuation and mass energy-absorption coefficients for H, C, N, O, Ar, and seven mixtures from 0.1 keV to 20 MeV. Radiat Res 70:58–81

ICRP (1983) Radionuclide transformations (publication 38). (Annals of the ICRP), p 25. Pergamon Press, Oxford

ICRP (1991) Recommendiation of the International Commission on Radiological Protection (publication 60). Pergamon Press, Oxford

ICRU (1983) Report 36. Microdosimetry. International Commission of Radiation Units and Measurements, Bethesdy
ICRU (1986) The quality factor in radiation protection. (Report 40) International Commission of Radiation Units and Measurements, Bethesda
Kellerer AM (1968) Local energy spectra and counter resolution. Ann Res Report NYO-2750-5 P-40:94–103
Kellerer AM (1968) Mikrodosimetrie, Grundlagen einer Theorie der Strahlenqualität. (GSF Ser. Monogr. B1) Gesellschaft für Strahlenforschung, Munich
Kellerer AM, Rossi HH (1984) On the determination of microdosimetric parameters in time-varying radiation fields: the variance-covariance method. Radiat Res 97:237–245
Kliauga P, Rossi HH, Johnson G (1987) A multi-element proportional counter for radiation protection measurements. Radial Res Lab Univ Columbia, pp 95–103
Larkins FP (1977) Semiempirical Auger-electron energies for elements $10 < Z < 100$. Atomic Data Nucl Data Tables 20:311–387
Lederer CM, Shirley VS (1978) Table of isotopes. Wiley, New York, p 81
NCRP (1991) Conceptual basis for calculations of absorbed dose distributions. (Report 108) National Council on Radiation Protection and Measurements, Bethesda
Rossi HH (1983) Multi-element dosimeters for radiation protection measurements. Health Phys 44:403–404
Rossi HH (1984) Development of microdosimetric counters, past, present and future. Radiat Prot Dosim 9:161–168
Seltzer SM (1993) Calculation of photon mass energy-transfer and mass energy-absorption coefficients. Radiat Res 136:147–170
Srdoc D (1979) The response of the proportional counter to unit charge. TIS USDE, Progress Report COO-4733-II, PM-1, pp 65–71
Waibel E, Grosswendt B (1992) W values and other transport data on low energy electrons in tissue equivalent gas. Phys. Med. Biol 37:1127–1145